University of Pennsylvania
ScholarlyCommons

Department of Physics Papers   Department of Physics

DNA-decorated carbon nanotube-based FETs as ultrasensitive chemical sensors: Discrimination of homologues, structural isomers, and optical isomers

S. M. Khamis
University of Pennsylvania

R. A. Jones
University of Pennsylvania

A.T. Charlie Johnson Jr.
University of Pennsylvania, cjohnson@physics.upenn.edu

G. Preti
Monell Chemical Senses Center, University of Pennsylvania

J. Kwak
Monell Chemical Sense Center

See next page for additional authors

Follow this and additional works at: http://repository.upenn.edu/physics_papers

Part of the Physics Commons

Recommended Citation

Khamis, S. M., Jones, R. A., Johnson, A., Preti, G., Kwak, J., & Gelperin, A. (2012). DNA-decorated carbon nanotube-based FETs as ultrasensitive chemical sensors: Discrimination of homologues, structural isomers, and optical isomers. Retrieved from http://repository.upenn.edu/physics_papers/244

DNA-decorated carbon nanotube-based FETs as ultrasensitive chemical sensors: Discrimination of homologues, structural isomers, and optical isomers

Abstract

We have explored the abilities of all-electronic DNA-carbon nanotube (DNA-NT) vapor sensors to discriminate very similar classes of molecules. We screened hundreds of DNA-NT devices against a panel of compounds chosen because of their similarities. We demonstrated that DNA-NT vapor sensors readily discriminate between series of chemical homologues that differ by single methyl groups. DNA-NT devices also discriminate among structural isomers and optical isomers, a trait common in biological olfactory systems, but only recently demonstrated for electronic FET based chemical sensors.

Author(s)

S. M. Khamis, R. A. Jones, A.T. Charlie Johnson Jr., G. Preti, J. Kwak, and A. Gelperin

DNA-decorated carbon nanotube-based FETs as ultrasensitive chemical sensors: Discrimination of homologues, structural isomers, and optical isomers

S. M. Khamis,[1,a] R. A. Jones,[1] A. T. C. Johnson,[1,b] G. Preti,[2,3] J. Kwak,[2] and A. Gelperin[2,4,b]

[1]*Department of Physics and Astronomy, University of Pennsylvania, Philadelphia, Pennsylvania 19104, USA*
[2]*Monell Chemical Senses Center, Philadelphia, Pennsylvania 19104, USA*
[3]*Department of Dermatology, University of Pennsylvania, Philadelphia, Pennsylvania 19104 USA*
[4]*Princeton Neuroscience Institute, Department of Molecular Biology, Princeton University, Princeton, New Jersey 08544, USA*

We have explored the abilities of all-electronic DNA-carbon nanotube (DNA-NT) vapor sensors to discriminate very similar classes of molecules. We screened hundreds of DNA-NT devices against a panel of compounds chosen because of their similarities. We demonstrated that DNA-NT vapor sensors readily discriminate between series of chemical homologues that differ by single methyl groups. DNA-NT devices also discriminate among structural isomers and optical isomers, a trait common in biological olfactory systems, but only recently demonstrated for electronic FET based chemical sensors. *Copyright 2012 Author(s). This article is distributed under a Creative Commons Attribution 3.0 Unported License.* [http://dx.doi.org/10.1063/1.4705394]

I. INTRODUCTION

DNA is an informational biopolymer whose complex secondary structure enables high affinity interactions with a range of ligands, including water,[1–3] ions,[2,4–6] hormones,[7,8] proteins,[9–11] transcription factors,[12,13] dyes,[14,15] enzymes,[16] and vapor-phase odorants.[17,18] We have combined the combinatorial complexity and precise polymer engineering of single-stranded DNA with the exquisite electrical sensitivity of field effect transistors consisting of individual semiconducting single-walled carbon nanotubes (NTs)[19,20] to create a new sensor technology for both aqueous and vapor-phase analytes.[21] The DNA-decorated NT sensors can be tuned for detection of a wide variety of analytes by selection of the base sequence of the DNA applied to the surface of the NTs.[22] DNA-NT hybrid sensors have potential utility for understanding the physics of ligand-DNA interactions[23,24] and contributing to the development of a new generation of devices for electronic olfaction.[25,26] In earlier reports we demonstrated that DNA-NT have a number of favorable properties for use in electronic olfaction including rapid response and full recovery to baseline (seconds), sensitivity to many common odorants at low concentration (ppb to ppm level), and chemical responses that are controlled by the DNA base sequence.

Here we show that DNA-NT sensors have the ability to discriminate between members of a homologous series of vapor-phase analytes differing by single methylene units as well as between structural isomers and pairs of enantiomers (molecules that are non-superimposable mirror images of each other). The discrimination of enantiomers is a remarkable characteristic found in living

---

[a]Present address: Adamant Technologies, San Francisco CA 94110, USA
[b]Authors to whom correspondence should be addressed. Email: cjohnson@physics.upenn.edu, gelperin@princeton.edu
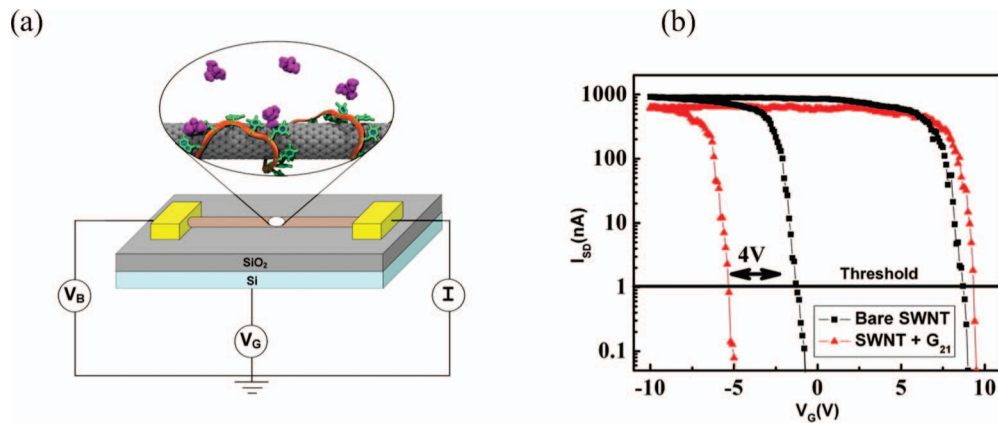
FIG. 1. (a) Schematic of the DNA-NT vapor sensor. (b) Typical I-V_G characteristics for a bare NT FET (black data) and the same device after functionalization with DNA sequence G_{21}, defined in Table I in the main text.

olfactory systems[27–29] and some sensor modalities.[30–35] Additionally, we show sensor responses to a gaseous analyte, dimethylsulfone, to which the human olfactory system is insensitive.

II. MATERIALS AND METHODS

Sample fabrication methods are carefully designed to insure that devices consist of single- or few-nanotube FETs coated with a uniform, nanoscale layer of DNA of a desired base sequence (Fig. 1(a)).

Single-walled carbon nanotubes (NTs) were grown by catalytic chemical vapor deposition (CVD) on a SiO$_2$/Si substrate. FET circuits were fabricated with Cr/Au source and drain electrodes patterned using optical lithography and the degenerately doped silicon substrate used as a backgate. Devices were fabricated using a resist bilayer process that we have demonstrated yields FET devices with excellent electrical characteristics comparable to the best reports of devices fabricated with electron beam lithography.[36,37] For each device, source-drain current I$_{SD}$ was measured as a function of bias voltage V$_B$ and gate voltage V$_G$ under ambient laboratory conditions (Fig. 1(b)). Circuits consisting of individual p-type semiconducting nanotubes, where the carriers are positively charged holes, were selected by using only devices that showed a strong decrease in I(V$_G$) for positive V$_G$ (ON/OFF ratio exceeding 1000) as well as an on-state resistance of less than 1MΩ, indicative of high quality devices with pristine surface chemistries.

Base sequences of the ssDNA oligomers used in these experiments are listed in Table I. Sequences Seq 1 and Seq 2 were chosen initially based on prior work.[38,39] Additional sequences consisting of repeats of single bases or pairs of bases as well as reordered version of Seq 1 and Seq 2 were also studied, and responses of as-fabricated (bare) NT devices were measured. Although the total number of sequences tested to date is only 16, we believe that the vapor response properties discussed below are characteristic of DNA-NT based on broad classes of ssDNA sequences.

Oligonucleotides were obtained from Invitrogen (Carlsbad, CA) and diluted in deionized ultrafiltered water to make stock solutions of 100 μM. Nanotube FETs were non-covalently functionalized with the appropriate DNA oligomer by incubation in a 10μL drop of a solution containing DNA of the desired sequence for 45-60 min, which enables the self-assembly of a 1 − 2 nm thick layer of DNA on the device, as determined by Atomic Force Microscopy.[21,40] During this step, the sample is kept in an environment of 100% relative humidity, and after incubation the drop is physically removed by blowing with a stream of clean nitrogen gas. This prevents drying of the drop of DNA solution, which leads to deposition of excessive DNA on the sample. We have found that samples with thick (micrometers) layers of DNA show no measurable sensor responses. The non-covalent functionalization scheme described above ensures that the intrinsic electronic properties of the NT FET are preserved.

TABLE I. Nucleotide sequences that were studied in the experiments described here. The naming conventions are used in Figure 8 below. "Seq 2 Soup" consists of a mixture of single nucleotides in the same relative concentrations as found in Seq 2. Seq 1RNA and Seq 2 RNA are RNA molecules.

Bare	as fabricated with no DNA applied
Seq 1	5' GAG TCT GTG GAG GAG GTA GTC 3'
Seq 1α	5' AAA ACC GGG GGG GGG GTT TTT 3'
Seq 1RNA	5' GAG UCU GUG GAG GAG GUA GUC 3'
Seq 1R1	5' CGA GGG AGT TGT ACT TGG AGG 3'
Seq 1R2	5' TGA TGT GGG TGC CGA AGG TGA 3'
Seq 2	5' CTT CTG TCT TGA TGT TTG TCA AAC 3'
Seq 2α	5' AAA ACC CCC GGG GTT TTT TTT TTT 3'
Seq 2 Soup	4dATP : 5dCTP : 4dGTP : 11dTTP
Seq 2RNA	5' CUU CUG UCU UGA UGU UUG UCA AAC 3'
Seq 2R1	5' TAC TGT CTC ATT CTG GAT ATT CTG 3'
Seq 2R2	5' GAA TAT GTA CTT GTC CCT GTT CTT 3'
GT$_{12}$	5' GTG TGT GTG TGT GTG TGT GTG TGT 3'
A$_{21}$	5' AAA AAA AAA AAA AAA AAA AAA 3'
C$_{21}$	5' CCC CCC CCC CCC CCC CCC CCC 3'
G$_{21}$	5' GGG GGG GGG GGG GGG GGG GGG 3'
T$_{21}$	5' TTT TTT TTT TTT TTT TTT TTT 3'

Five to twenty devices from multiple different NT growth runs were selected for detailed analysis and treated with DNA for each of the discrimination experiments described below. The total number of devices used for the results presented in Fig. 8 is roughly 600. For all sequences used, application of DNA caused the threshold value of V_G for measurable conduction to decrease by 4 ± 1 V (Fig. 1(b)), corresponding to a hole density decrease of roughly 400 μm, assuming a backgate capacitance of 25 aF/μm, typical for this device geometry.[41] Furthermore, the "ON" state conductivity of the DNA-NT was typically ~10-30% lower than that of the bare device, suggesting weak carrier scattering by the molecular coating.

For vapor response measurements, gas flows containing analyte vapors of known concentration were created using a computer-controlled bubbler system as described previously.[42, 43] A high purity carrier gas was used to flush the device between exposure to analyte-containing gas flows. Nitrogen, argon and "Zero Air" (GTS-Welco) have all been used as carrier gases with essentially identical results. Care is taken to maintain a constant flow rate across the devices throughout all gas sensing experiments, so that we remove any chance of false signals that could arise from flow rate variations. The humidity of the gas stream may also be controlled using the bubbler system. Measured device responses are constant for relative humidity levels $0 - 80$ % (data not shown).

Gas Chromatography-Mass Spectrometry (GC/MS). A Thermoquest GC/MS with Xcalibur software (ThermoElectron Corp., San Jose, CA) was used for all analyses. A polar, Stabilwax column, 30M x 0.32mm with 1.0μ coating, (Restek Corp., Bellefonte, PA) was used for separation. Helium carrier gas was used at a constant column flow rate of 2.5 ml/minute throughout the analysis.

Injections were made into the chromatograph's injector that was heated to 230°C. GC conditions were as follows: initial column temperature 60°C was held for 4 minutes; then temperature programmed at 6°C/min. to a final temperature of 220°C.

Data acquisition and operating parameters for the mass spectrometer were set as follows: scan rate 2/sec; scan range *m/z* 41 to *m/z* 440; ion source temperature 200°C; ionizing energy 70eV.

Quantification of Dimethylsulfone in the Vapor Phase. A solution of dimethylsulfone (DMSO$_2$) was prepared by dissolving 0.05 grams of DMSO$_2$ (Sigma-Aldrich) in 100ml (102 grams) of dipropylene glycol. This yielded a solution of 490 parts-per-million (ppm) by weight of DMSO$_2$. To measure the concentration of DMSO$_2$ present in the headspace above this solution at room temperature (~24°C), 1 milliliter (ml) of the solution was transferred to a 22 ml vial, sealed with a Teflon-coated silicon septum for syringe insertion. The vial with solution was agitated for 20 min using a magnetic stir bar prior to the insertion of a 10 μl gas-tight syringe. The syringe plunger was

withdrawn and inserted ("pumped") three times and a sample of $5\mu l$ was withdrawn for injection into the gas chromatograph-mass spectrometer system (GC/MS).

This process was repeated 3 times to obtain a mean level of DMSO$_2$, as a peak area. This peak area was converted to an absolute amount of DMSO2 using a standard curve for this compound, generated as follows.

A calibration curve in the concentration ranges of interest was obtained by diluting a stock solution of 0.1mg/ml of DMSO$_2$ in CHCl$_3$. The following solutions were used containing DMSO$_2$ concentrations of 0.01mg/ml, 0.001mg/ml, 0.00025mg/ml and 0.00005mg/ml. Each solution was analyzed a minimum of 3 times to create a calibration curve of peak area vs. concentration.

Selection of analytes for the measurements described here was guided by several considerations. First, we wanted to explore the responses of this new class of sensors to components of human body odors, a longstanding interest in our laboratories.[44, 45] Second, we wanted to challenge our new sensor technology with analytes that would potentially reveal new insights into the mechanism of the analyte-DNA-nanotube interaction underlying the observed changes in conductance during analyte application. Third, we also wanted to determine if the new sensor technology can discriminate between nearly identical analytes such as optical isomers, which is a discrimination typical of biological olfaction.[46, 47]

III. RESULTS AND DISCUSSION

Although there have been many investigations of the chemical detection properties of functionalized carbon nanotube transistors, current understanding of the response mechanism is primarily qualitative. We assume that the mechanism underlying changes in NT conduction is dominated by electrostatic coupling to the local environment, which consists of adsorbed single stranded DNA, a nanoscale hydration layer, and any molecules bound from the vapor phase. Shifts in threshold gate voltage for conduction are attributed to changes in the effective charge in NT environment, while variation in the on-state current is assumed to reflect changes in carrier scattering. The DNA layer is bound to the NT by the attractive π-π stacking interactions between the DNA bases and the NT sidewall.[48, 49] Although the bases are primarily flush with the NT, thermal fluctuations lead to a significant number of them being desorbed.[50] We hypothesize that this results in a complex set of binding pockets, specific to the base sequence of the DNA and located within 1-2 nm of the NT surface. When odorant molecules are solvated by the hydration layer and bound in these pockets, the conductance of the NT devices is altered, which we assume reflects changes in carrier density and carrier scattering associated with the electrostatic potential at the NT sidewall. These changes can occur even for the case of odorant molecules that should remain *uncharged* in the hydration layer, as is also reported for other sorts of functionalized NT devices.[51]

The first indication that DNA-NT devices possess significant discriminative power between closely related analytes came from responses to a set of homologous carboxylic acids, with structures shown in Fig. 2(a). As shown in Fig. 3(a), application of propanoic acid (C$_3$H$_6$O$_2$), hexanoic acid (C$_6$H$_{12}$O$_2$) and octanoic acid (C$_8$H$_{16}$O$_2$) to a sensor coated with Seq. 1 (refer to Table I for nucleotide sequences) gave distinctly different concentration-response profiles. As is typically done to account for device-to-device variation in nano-enabled sensor systems, responses are shown as percent change in conductance upon analyte application relative to conductance under pure carrier gas flow. We note that the threshold of detection for each analyte is correlated with the solubility of each molecule in water, ranging from propanoic acid that is miscible with water, hexanoic acid with solubility 11000 mg/L to octanoic acid at just 790 mg/L. This aspect will be discussed further below.

The aldehydes octanal, nonanal and decanal (see Fig. 2(b)) were chosen as a second example of a homologous series. Figure 3(b) displays data from sensors coated with Seq 1, as they were exposed to octanal, nonanal and decanal at nominal concentrations spanning the range 0.01 – 50% of saturated vapor. These compounds follow the same trend as the carboxylic acids in that the threshold of response is correlated to the solubility of each compound in water. Interestingly, decanal, which is insoluble in water, causes a response that is opposite in sign to that of the smaller aldehydes that are soluble and no response is observed at vapor concentrations below 10%. We propose a mechanism where the change in conductance reflects the electrostatic influence of its dipole moment (roughly 3

(a)   (b)   (c)

Propanoic acid   Octanal   4-Methyl Pentanoic Acid

Hexanoic acid   Nonanal   2-Methyl Pentanoic Acid

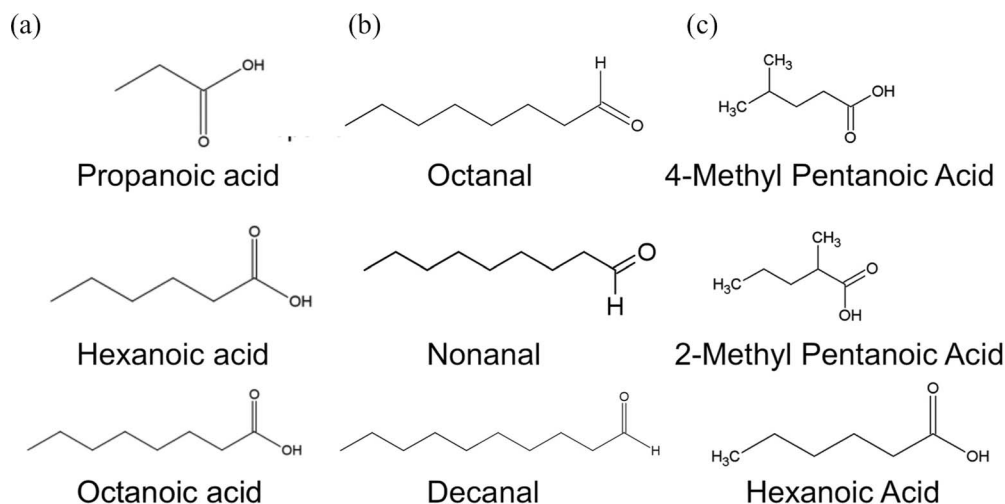Octanoic acid   Decanal   Hexanoic Acid

FIG. 2. (a) Structures of three homologous carboxylic acids used to elicit responses from DNA-NT sensors. (b) Structures of three aldehydes that were tested. (c) Structures of structural isomers tested against DNA-NT devices.
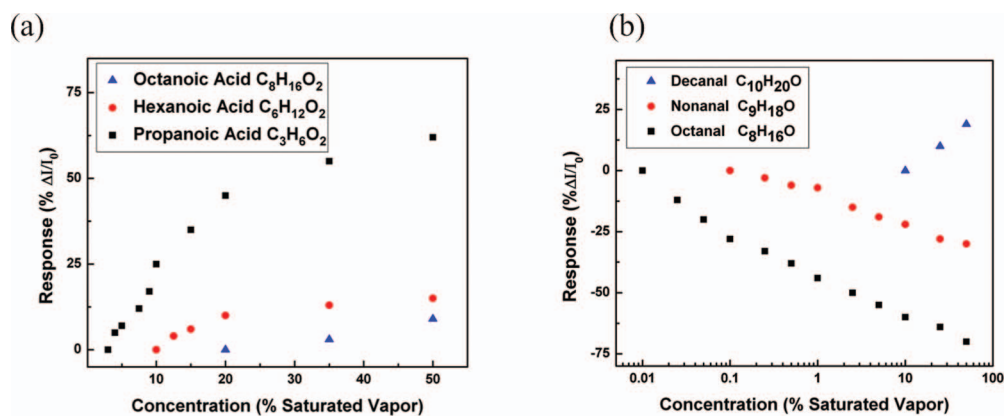
FIG. 3. (a) Responses of DNA-NT sensors coated with Seq. 1 to carboxylic acids with carbon chain lengths from C3 to C8. (b) Responses of DNA-NT sensors coated with Seq. 2 to a series of homologous aldehydes.

Debye for octanal). For the case of octanal and nonanal, the molecule is solubilized, and the dipole has a preferred orientation with respect to the NT. For decanal, the molecule is forced to reside on the exterior of the hydration layer, and the dipole orientation is reversed, thereby reversing the sign of the conductance change.

N-Hexanoic acid, 2-methyl pentanoic acid, and 4-methyl pentanoic acid are structural isomers, with the same number of carbon, hydrogen and oxygen atoms ($C_6H_{12}O_2$) but arrayed as either a straight or branched carbon chain (Fig. 2(c)). DNA-NT coated with DNA Seq. 1 responds differentially to the straight chain compared to the branched isomers, with detection thresholds differing by three orders of magnitude (Fig. 4). The two branched-chain isomers present the same responses up to about 40% of saturated vapor pressure, beyond which point they are discriminable. Very different behavior is seen for DNA-NT devices based on Seq 2, which discriminate readily between the two branched isomers down to the lowest measured concentrations of roughly 300 ppb.

The water solubility of 2-methyl pentanoic acid (13000 mg/L) is similar to that of n-hexanoic acid (11000 mg/L), while 4-methyl pentanoic acid is essentially insoluble. Thus the geometry of the branched-chain isomers appears to play a more important role than water solubility in the responses of the DNA-NT to these isomers. Further, despite the small difference in solubility between n-hexanoic acid and 2-methyl pentanoic acid, their detection thresholds differ by more than a factor of 100. In contrast, the solubilities of n-hexanoic acid and n-octanoic acid differ by more (nearly
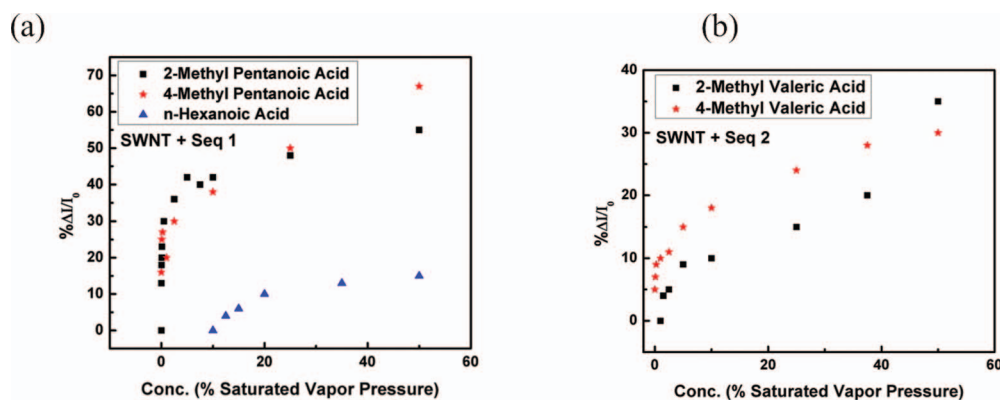
FIG. 4. (a) DNA-NT based on Seq 1 responds differentially to the straight chain n-hexanoic acid compared to the branched isomers. (b) DNA-NT based on Seq 2 discriminate readily between the two branched isomers down to the lowest tested concentration of roughly 300 ppb.
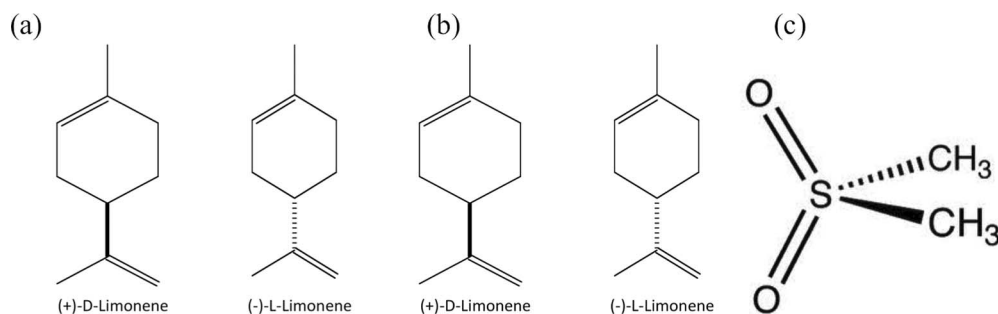

FIG. 5. (a) Structures of the enantiomers of limonene. (b) Structures of the enantiomers of carvone. (c) Structure of dimethyl sulfone, referred to as "DMSO$_2$" in the text.

10000 mg/L), while the difference in their response thresholds is only a factor of two. This suggests that the molecular geometry of the odorant being tested has an enormous affect on its ability of to affect conduction in DNA-NT devices. This concept will be discussed further below.

A further test of the ability of DNA-NT sensors to discriminate between closely related compounds is afforded by testing for responses to pairs of enantiomers, which differ only in the three-dimensional shape of the members of the pairs[52] although each member of the pair of enantiomers typically has a distinct odor.[28,53] We tested enantiomers of limonene and carvone, whose structures are shown in Figs. 5(a) and 5(b). First tests were done on DNA-NT based on Seq 1 and Seq 2, with analyte concentrations from 0.01 to 50% of saturated vapor (∼ 300 ppb – 1500 ppm for limonene, and 50 ppb – 250 ppm for carvone). As shown in Figs. 6(a) and 6(b), DNA-NT based on Seq 1 showed very different responses to the limonene enantiomers, while responses from DNA-NT based on Seq 2 were very similar. DNA-NT based on Seq 1 also showed differential responses to the carvone enantiomers, although the differences were not as strong as was seen for limonene (Fig. 7(a)).

Given that nucleotide Seq. 1 displayed distinctively different responses to the enantiomers of limonene, we created DNA-NT devices based on two random permutations of nucleotide sequences based on Seq. 1, designated Seq. 1R1 and Seq. 1R2. Both permutations of Seq. 1 also gave very different response patterns to the enantiomers of limonene over more than two orders of magnitude of concentration (Figs. 6(c) and 6(d)). These results will be informative in modeling of the analyte-oligomer interactions underlying the measured responses. This experiment provides a dramatic example of how the geometry of the analyte molecule has a large impact on the sensor response, similar to the results obtained for geometric isomers of n-hexanoic acid.
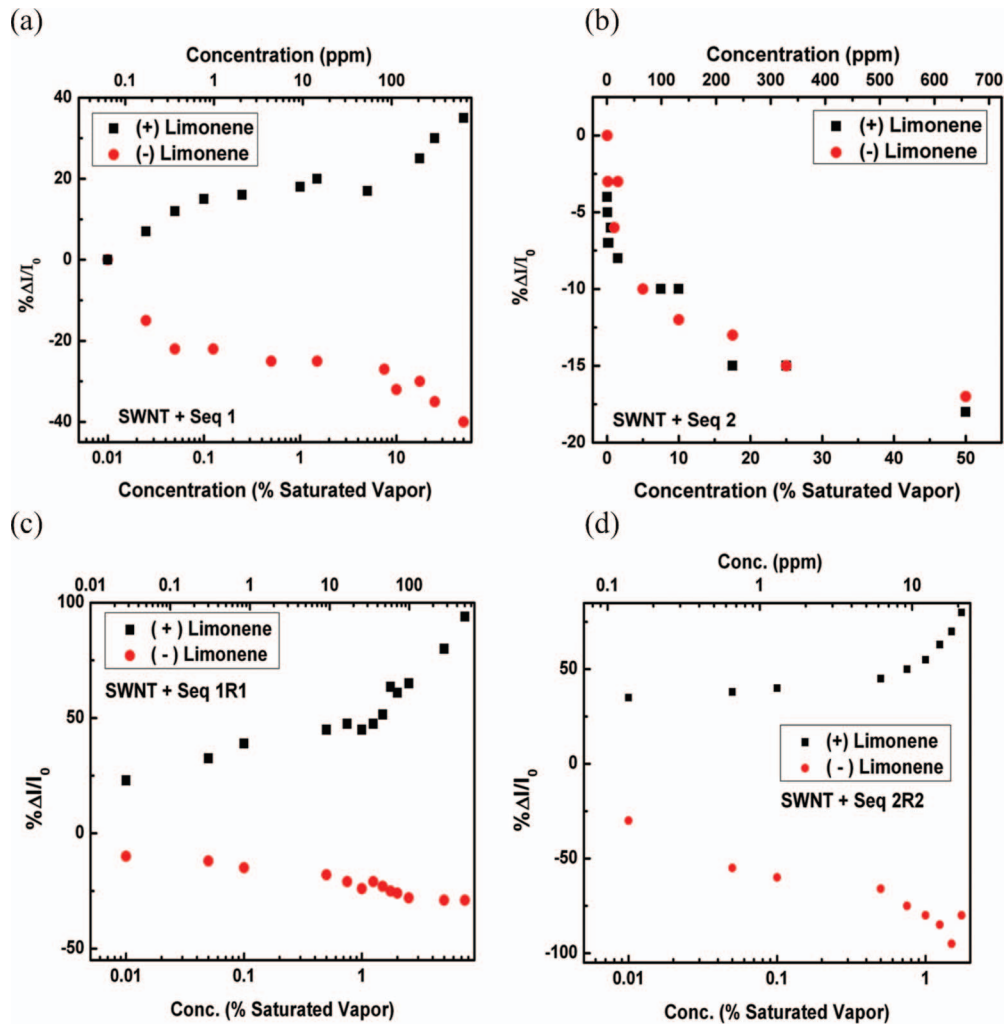
FIG. 6. (a) DNA-NT devices based on Seq 1 readily discriminate between the different enantiomers of limonene. (b) In contrast, almost no differentiation was observed for DNA-NT based on Seq 2. (c, d) DNA-NT based on randomized variants of Seq 1 and Seq 2 (Seq1R1 and Seq 2R2, see Table I) showed strong differentiation between the enantiomers of limonene.
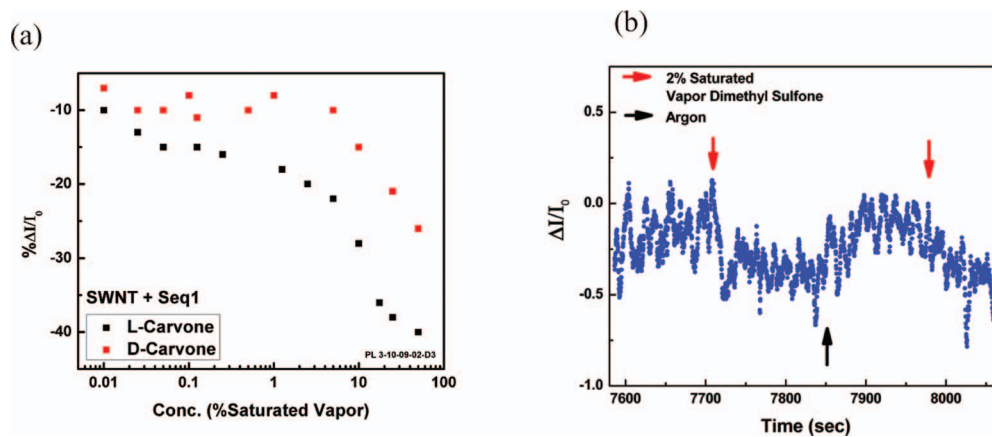

FIG. 7. (a) DNA-NT based on Seq 1 discriminates between the enantiomers of carvone. (b) Identical devices also respond upon exposure to 25 ppb of dimethylsulfone, a compound that is odorless to humans.

All Measurements Performed at 3% Saturated Vapor Pressure • Detectable at Higher Concentration • Quoted values represent average of 5-20 measured devices	Bare	Seq1	Seq1 α	Seq1 RNA	Seq1R1	Seq2	Seq2α	Seq 2 Soup	Seq2R1	Seq2R2	Seq2 RNA	GT12	A21	C21	G21	T21
Propionic Acid	0±1	+17±2	0±1	+45±10		+8±1	+10±3	0±1			+40±5	0±1	0±1	0±1	0±1	0±1
Hexanoic Acid		0±4 *														
Octanoic Acid		0±4 *														
2-Methyl Valeric Acid	3±2	35±7				5±3										
4-Methyl Valeric Acid	0±3	30±5				12±4										
n-Octanal		-50±5														
n-Nonanal		-13±5														
n-Decanal		0±4 *														
DMMP	0±1	-14±2	0±1	+30±5		-7±2	-15±2	0±1			-35±10	0±1	0±1	0±1	0±1	0±1
DNT	0±1	-14±4	0±1	-20±5		-4±2	0±4	0±1			-70±10	0±1	0±1	0±1	0±1	0±1
(+) Limonene	5±2	13±4			50±7	40±8			80±8	60±8						
(-) Limonene	-7±3	-7±4			-30±5	6±3			-65±9	-80±10						
L-Carvone	-7±4	-20±5				-10±4										
D-Carvone	-8±4	-10±5				-15±5										
Methanol	0±1	-12±2	-50±2	32±5		-20±2	8±1	-60±4			20±5	-4±2	-15±2	0±1	-50±2	0±1
Trimethylamine	-9±2	-20±2	-20±3	-40±10		-30±2	14±2	-25±5			-45±5	-50±5	-25±3	-16±5	-50±6	-10±6
Dimethyl sulfone (500ppm)		50±10														

FIG. 8. A large number of DNA-NT sensor responses demonstrating how responses vary with the DNA sequence. Red shades denote positive changes in (normalized) conductance while blue shades denote negative changes in conductance.

Finally, we considered the case of a volatile compound that is "odorless" to humans, *i.e.*, it does not elicit an olfactory sensation in normal human subjects. Dimethylsulfone, whose structure is shown in Fig. 7(a), is a compound characteristic of the volatiles collected above human skin. We found that semiconducting nanotube sensors coated with DNA Seq 1 showed a small but clearly detectable response to dimethylsulfone at 2% of saturated vapor, a calculated concentration of 25 ppb (Fig. 7(b)). This demonstrates that this new sensor technology has sensing capabilities beyond those of the human olfactory system.

A summary of sensor response measurements made using a panel of 17 odorants applied to both bare nanotube sensor devices and DNA-NT based on one of 15 different nucleotide combinations is shown in Fig. 8. Although we have test results from only 95 of the 272 possible combinations, it is clear that DNA-NT based on a wide variety of both DNA and RNA nucleotide oligomers have the ability to respond to analyte vapors or have responses that differ strongly from that shown by uncoated nanotube sensors. Note that each cell in Fig. 8 represents between 15-30 distinct measurements of devices functionalized with the indicated DNA sequence, yielding statistically significant measurements for each of the observed sets of responses.

IV. DISCUSSION

An engineered sensor system for volatile analytes comprised of single-walled semiconducting carbon nanotubes fabricated as field-effect transistors and coated with DNA or RNA oligonucleotides can show rapid and selective responses to a variety of vapors, dependent on the base sequence of the oligonucleotide used to coat the nanotubes.[21,22] We now show that this sensor platform can discriminate between homologous series of analytes differing by a single carbon atom, between structural (also known as constitutional) isomers where the same collection of atoms are bonded together in different orders, and between pairs of enantiomers differing only in the three-dimensional shape of compositionally identical molecules. This degree of versatility provides for the creation of a sensor architecture to truly mimic that of mammalian olfaction. Many to many sensor to analyte interactions allow for fingerprint-like matching of a single analyte or mixture of analytes, while one to one sensor interactions, as is the case with the majority of chemical sensor architectures, do not allow for the pattern recognition that is necessary to screen for unknown concentrations of analytes in a changing background.[54]

Other sensor modalities have been shown to display stereo-specific sensing,[30–34,55] which is important for the detection of trace chiral impurities in commercial samples of uni-chiral compound[56] and the assessment of the enantioselective toxicology of drugs[57] and pesticides.[58,59] These interactions will also be important for creating sensors for detection of chemicals and the production facilities of chemicals such as methamphetamines where the dextrorotary enantiomer "crystal meth" is a highly addictive street drug, while its levorotary enantiomer is an over-the-counter drug used in nasal decongestants.

Understanding stereospecific interactions of chiral species with DNA and RNA is of direct relevance to understanding the mode of action of DNA-binding drugs, however, most the research on this topic uses double-stranded rather than single-stranded DNA.[60] Plasmid DNA has been shown to interact differentially with gold surfaces coated with the enantiomers of N-isobutyryl-cysteine[61] but this stereospecific binding may not generalize to surfaces covered with single-stranded DNA oligomers such as those used in our experiments shown in Table I. It has, however, been shown that short DNA oligomers composed of only four nucleotides can show stereospecific interactions with the enantiomers of alpha-amino acids.[62] Further modeling work using the approach taken in our previous studies of DNA interactions with the surfaces of carbon nanotubes[40,63,64] will be critical to making testable hypotheses about the molecular mechanisms of enantiomer discrimination by DNA-coated nanotube sensors.

Measurements of some straight-chained carboxylic acids emanating from human skin are available but no measurements have been published of normal levels of characteristic axillary odorants, however, estimations can be made as follows. The concentrations of axillary odorants, including carboxylic acids like those shown in Fig. 2(a), are likely to be in the range from 100's of nanograms to 100's of micrograms per gm of sweat. If we take the high estimate (100 μg/gm sweat or 100 ppm) and if 0.1-1.0% of this material evaporates into the vapor phase, the final concentration is $0.1 - 1.0$ ppm, within the detection limit of DNA-NT devices. However, at the low end of the estimated concentration of axillary volatiles, (100 ng/gm sweat), the concentration would be 0.1 - 1.0 ppb. Detection of axillary odorants at this level would require selection of a DNA sequence more efficacious at sensing axillary odorants than the ones tested thus far, likely augmented by summing the responses of many sensors to average out noise.

Volatile carboxylic acids are the most diverse and characteristic class of known axillary odorants and are released from proteinaceous precursors by the action of enzymes released by cutaneous bacteria.[65,66] In addition, the type and abundance of volatile carboxylic acids in the axillae is directly related to variants in the ABCC11 gene,[67,68] which may influence the amount of apocrine secretion binding proteins which carry odorants to the skin surface.[67]

Dimethylsulfone (DMSO2) is a mammalian metabolite derived from methanethiol metabolism via oxidation of dimethylsulfide.[69] It is found in mammalian body fluids including mouse and human urines[70,71] as well as human skin emanations.[44,72] Recent studies, reported in a preliminary fashion,[73] also suggest that the concentration of $DMSO_2$ increases significantly above skin sites invaded by basal cell carcinoma. $DMSO_2$ is an unusual volatile sulfur compound since it has no apparent odor, even at neat concentration. Consequently, while it is very amenable to detection using analytical techniques, the human olfactory system is blind to its presence. Here we have demonstrated that DNA-coated single-walled carbon nanotubes display extraordinary sensitivity to this compound which suggests that an electronic nose fitted with diverse DNA-coated single-walled carbon nanotube sensor arrays maybe prove to be more sensitive and selective than even the canine or murine olfactory systems for selective applications.

[1] S. H. Chen, L. Liu, X. Chu, Y. Zhang, E. Fratini, P. Baglioni, A. Faraone, and E. Mamontov, J Chem Phys **125**, 171103 (2006).
[2] S. Sen, D. Andreatta, S. Y. Ponomarev, D. L. Beveridge, and M. A. Berg, J Am Chem Soc **131**, 1724-35 (2009).

[3] T. Elsaesser, Biol Chem **390**, 1125-32 (2009).

[4] M. Feig and B. M. Pettitt, Biophys J **77**, 1769-81 (1999).

[5] C. K. Materese, A. Savelyev, and G. A. Papoian, J Am Chem Soc **131**, 15005-13 (2009).

[6] M. R. Gill, J. Garcia-Lara, S. J. Foster, C. Smythe, G. Battaglia, and J. A. Thomas, Nature Chemistry **1**, 662-667 (2009).

[7] N. Z. Lu, S. E. Wardell, K. L. Burnstein, D. Defranco, P. J. Fuller, V. Giguere, R. B. Hochberg, L. McKay, J. M. Renoir, N. L. Weigel, E. M. Wilson, D. P. McDonnell, and J. A. Cidlowski, Pharmacol Rev **58**, 782-97 (2006).

[8] T. Kino, Y. A. Su, and G. P. Chrousos, Cell Mol Life Sci **66**, 3435-48 (2009).

[9] T. Hu and B. I. Shklovskii, Phys Rev E Stat Nonlin Soft Matter Phys **76**, 051909 (2007).

[10] U. Kolthur-Seetharam, M. M. Pradeepa, N. Gupta, R. Narayanaswamy, and M. R. Rao, J Histochem Cytochem **57**, 951-62 (2009).

[11] A. Lachish-Zalait, C. K. Lau, B. Fichtman, E. Zimmerman, A. Harel, M. R. Gaylord, D. J. Forbes, and M. Elbaum, Traffic **10**, 1414-28 (2009).

[12] J. Zeng, X. Q. Cao, H. Zhao, and H. Yan, Phys Rev E Stat Nonlin Soft Matter Phys **80**, 041917 (2009).

[13] S. Hu, Z. Xie, A. Onishi, X. Yu, L. Jiang, J. Lin, H. S. Rho, C. Woodard, H. Wang, J. S. Jeong, S. Long, X. He, H. Wade, S. Blackshaw, J. Qian, and H. Zhu, Cell **139**, 610-22 (2009).

[14] M. Wanunu, J. Sutin, and A. Meller, Nano Lett **9**, 3498-502 (2009).

[15] L. J. Kricka and P. Fortina, Clin Chem **55**, 670-83 (2009).

[16] E. P. Mimitou and L. S. Symington, DNA Repair (Amst) **8**, 983-95 (2009).

[17] L. B. Williams, J. White, and J. S. Kauer, Chem Senses **31**, A47 (2006).

[18] J. White, K. Truesdell, L. B. Williams, M. S. Atkisson, and J. S. Kauer, PLoS Biol **6**, e9 (2008).

[19] D. E. Johnston, M. F. Islam, A. G. Yodh, and A. T. Johnson, Nat Mater **4**, 589-92 (2005).

[20] H. R. Byon, S. Kim, and H. C. Choi, Nano **3**, 415-431 (2008).

[21] C. Staii, A. T. Johnson, Jr., M. Chen, and A. Gelperin, Nano Lett **5**, 1774-8 (2005).

[22] A. T. Johnson, S. M. Khamis, G. Preti, J. Kwak, and A. Gelperin, IEEE Sensors J **10**, 159-166 (2010).

[23] S. Kim, T. G. Kim, H. R. Byon, H. J. Shin, C. Ban, and H. C. Choi, J Phys Chem B **113**, 12164-8 (2009).

[24] R. R. Johnson, A. Kohlmeyer, A. T. Johnson, and M. L. Klein, Nano Lett **9**, 537-41 (2009).

[25] P. Bondavalli, P. Legagneux, and D. Pribat, Sensors and Actuators B-Chemical **140**, 304-318 (2009).

[26] A. D. Wilson and M. Baietto, Sensors **9**, 5099-5148 (2009).

[27] C. Linster, B. A. Johnson, E. Yue, A. Morse, Z. Xu, E. E. Hingco, Y. Choi, M. Choi, A. Messiha, and M. Leon, J Neurosci **21**, 9837-43 (2001).

[28] B. Slotnick, Chem Senses **32**, 721-725 (2007).

[29] T. Clarin, S. Sandhu, and R. Apfelbach, Behav Brain Res **206**, 229-35 (2010).

[30] J. Ruta, C. Ravelet, I. Baussanne, J. L. Decout, and E. Peyrin, Anal Chem **79**, 4716-9 (2007).

[31] C. Xu, S. C. Ng, and H. S. Chan, Langmuir **24**, 9118-24 (2008).

[32] D. Vardanega, F. Picaud, and C. Girardet, J Chem Phys **130**, 114709 (2009).

[33] P. Kurzawski, V. Schurig, and A. Hierlemann, Anal Chem **81**, 9353-64 (2009).

[34] B. B. Prasad, R. Madhuri, M. P. Tiwari, and P. S. Sharma, Talanta **81**, 187-96 (2010).

[35] L. Torsi, G. M. Farinola, F. Marinelli, M. C. Tanese, O. H. Omar, L. Valli, F. Babudri, F. Palimsano, P. G. Zambonin, and F. Naso, Nature Materials **7**, 412-417 (2008).

[36] S. M. Khamis, R. A. Jones, and A. T. C. Johnson, AIP Advances **1**, 022106 (2011).

[37] S. M. Khamis, R. R. Johnson, Z. Luo, and A. T. C. Johnson, Journal of Physics and Chemistry of Solids **71**, 476-479 (2010).

[38] J. E. White, L. B. Williams, M. S. Atkisson, and J. S. Kauer, Assoc Chemoreception Sciences XXVI Annual Meeting Abstracts, 32 (2004).

[39] J. E. White and J. S. Kauer, US Patent App. 2004/0101851 (2004).

[40] S. A. Khamis, R. R. Johnson, Z. T. Luo, and A. T. C. Johnson, J Physics Chem Solids **71**, 476-479 (2010).

[41] M. Radosavljevic, M. Freitag, K. V. Thadani, and A. T. Johnson, Nano Letters **2**, 761-764 (2002).

[42] Y. P. Dan, Y. Y. Cao, T. E. Mallouk, A. T. Johnson, and S. Evoy, Sensors Actuators B-Chemical **125**, 55-59 (2007).

[43] Y. Dan, Y. Cao, T. E. Mallouk, S. Evoy, and A. T. Johnson, Nanotechnology **20**, 434014 (2009).

[44] M. Gallagher, C. J. Wysocki, J. J. Leyden, A. I. Spielman, X. Sun, and G. Preti, Br J Dermatol **159**, 780-91 (2008).

[45] G. Preti, E. Thaler, C. W. Hanson, M. Troy, J. Eades, and A. Gelperin, J Chromatogr B Analyt Technol Biomed Life Sci **877**, 2011-8 (2009).

[46] C. S. Sell, Angew Chem Int Ed Engl **45**, 6254-61 (2006).

[47] R. Bentley, Chem Rev **106**, 4099-112 (2006).

[48] R. R. Johnson, A. T. C. Johnson, and M. L. Klein, Nano Letters **8**, 69-75 (2008).

[49] R. R. Johnson, A. T. Johnson, and M. L. Klein, Small **6**, 31-34 (2010).

[50] R. R. Johnson, A. Kohlmeyer, A. T. C. Johnson, and M. L. Klein, Nano Letters **9**, 537-541 (2009).

[51] B. R. Goldsmith, J. J. Mitala, J. Josue, A. Castro, M. B. Lerner, T. H. Bayburt, S. M. Khamis, R. A. Jones, J. G. Brand, S. G. Sligar, C. W. Luetje, A. Gelperin, P. A. Rhodes, B. Discher, and A. T. C. Johnson, ACS Nano **5**, 5408-5416 (2011).

[52] J. C. Brookes, A. P. Horsfield, and A. M. Stoneham, J R Soc Interface **6**, 75-86 (2009).

[53] M. Laska and G. M. Shepherd, Neuroscience **144**, 295-301 (2007).

[54] J. J. Hopfield, Proc Natl Acad Sci U S A **79**, 2554-8 (1982).

[55] X. He, X. Cui, M. S. Li, L. L. Lin, X. H. Liu, and X. M. Feng, Tetrahedon Lett **50**, 5853-5856 (2009).

[56] A. Henning and S. Matile, Chirality **21**, 145-51 (2009).

[57] H. Liu, L. Xu, M. Zhao, W. Liu, C. Zhang, and S. Zhou, Toxicology **261**, 119-25 (2009).

[58] J. K. Stanley and B. W. Brooks, Integr Environ Assess Manag **5**, 364-73 (2009).

[59] J. Ye, M. Zhao, J. Liu, and W. Liu, Environ Pollut **158**, 2371-83 (2010s).

[60] R. Corradini, S. Sforza, T. Tedeschi, and R. Marchelli, Chirality **19**, 269-94 (2007).

[61] H. Gan, K. Tang, T. Sun, M. Hirtz, Y. Li, L. Chi, S. Butz, and H. Fuchs, Angew Chem Int Ed Engl **48**, 5282-6 (2009).

[62] T. Sivaleela, M. R. Kumar, S. Prabhakar, G. Bhaskar, and M. Vairamani, Rapid Commun Mass Spectrom **22**, 204-10 (2008).

[63] R. R. Johnson, A. T. Johnson, and M. L. Klein, Nano Lett **8**, 69-75 (2008).

[64] R. R. Johnson, A. T. Johnson, and M. L. Klein, Small **6**, 31-4 (2010).

[65] X.-N. Zeng, J. J. Leyden, J. G. Brand, A. I. Spielman, K. J. McGinley, and G. Preti, J Chem Ecol **18**, 1039-1055 (1992).

[66] A. Natsch, F. Kuhn, and J. M. Tiercy, J Chem Ecol **36**, 837-46 (2010).

[67] G. Preti and J. J. Leyden, J Invest Dermatol **130**, 344-6 (2010).

[68] A. Martin, M. Saathoff, F. Kuhn, H. Max, L. Terstegen, and A. Natsch, J Invest Dermatol **130**, 529-40 (2010).

[69] U. F. Engelke, A. Tangerman, M. A. Willemsen, D. Moskau, S. Loss, S. H. Mudd, and R. A. Wevers, NMR Biomed **18**, 331-6 (2005).

[70] A. G. Singer, G. K. Beauchamp, and K. Yamazaki, Proc Natl Acad Sci U S A **94**, 2210-4 (1997).

[71] A. Takeuchi, S. Yamamoto, R. Narai, M. Nishida, M. Yashiki, N. Sakui, and A. Namera, Biomed Chromatogr **24**, 465-71 (2010).

[72] X.-N. Zeng, J. J. Leyden, A. I. Spielman, and G. Preti, J Chem Ecol **22**, 237-257 (1996).

[73] G. Preti, M. Gallagher, S. S. Fakharzadeh, C. J. Wysocki, J. Kwak, J. Marmion, H. Ozdener, C. J. Miller, C. D. Schmults, A. I. Spielman, X. M. Sun, and S. Chachkin, Chem Senses **33**, S138-S139 (2008).